INVERSE PROBLEM OF FLUID TEMPERATURE ESTIMATION INSIDE A FLAT MINI-CHANNEL STARTING FROM TEMPERATURE MEASUREMENTS OVER ITS EXTERNAL WALLS

Yassine Rouizi, D. Maillet, Y. Jannot, I Perry

European Congress on Computational Methods
in Applied Sciences and Engineering (ECCOMAS 2012)
J. Eberhardsteiner et.al. (eds.)
Vienna, Austria, September 10-14, 2012

INVERSE PROBLEM OF FLUID TEMPERATURE ESTIMATION INSIDE A FLAT MINI-CHANNEL STARTING FROM TEMPERATURE MEASUREMENTS OVER ITS EXTERNAL WALLS

Y. Rouizi[1], **D. Maillet**[1], **Y. Jannot**[1] **and I. Perry**[1]

[1]Laboratoire d'Energtique et de Mécanique Théorique Appliquée (LEMTA), Université de Lorraine
and CNRS, Vandoeuvre-lès Nancy, France
address
yassine.rouizi@ensem.inpl-nancy.fr
denis.maillet@ensem.inpl-nancy.fr
yves.jannot@ensem.inpl-nancy.fr
isabelle.perry@ensem.inpl-nancy.fr

Keywords: mini-channel, inverse problems, conduction and advection, infrared thermography

Abstract. *Modelling fluid flow and heat transfer inside a mini- or micro-channel constitutes a challenge because it requires taking into account many effects that do not occur in traditional macrostructured systems. In a mini-channel, presence of solid walls, whose volume fraction is not negligible, modifies heat diffusion (conjugated heat transfer): this means that traditional Nusselt correlations for forced convection have to be revisited, because the heat flux distribution at the wall is not always normal to it and the location of the heat source modifies the distribution of the heat transfer coefficient in the flow direction. Our objective is to characterize the mean velocity U and the heat transfer coefficient of external exchange h and to describe the bulk temperature distribution $T_b(x)$. The inverse method makes it possible to go back to this information starting from measurement of the temperature fields on the two external faces of the channel and a corresponding model through the minimization of a criterion. In this work, the temperature fields can be obtained either by a numerical model or by an experimental model by infrared thermography. Before an experimental validation by infrared thermography, we perform numerical simulations and a sensitivity analysis of the external temperature fields to the mean flow velocity U and to the external heat transfer coefficient h. The temperature and flux distributions over the internal faces of the walls are estimated by an inverse method then.*

1 INTRODUCTION

Modelling fluid flow and heat transfer inside a mini- or micro-channel constitutes a challenge because it requires taking into account many effects that do not occur in traditional macro-structured systems [8]. In a mini-channel, presence of solid walls, whose volume fraction is not negligible, modifies heat transfer and can induce axial conduction effects in the channel walls. These are generally neglected in the macro-systems [4, 6].

This study concerns the numerical and experimental modelling of both single phase water flow and heat transfer (conduction and advection) in a flat mini-channel (see figure 1). The flowing fluid layer (1 mm thickness) is located between two parallel polycarbonate solid walls (1 and 2 mm thicknesses). This material has been chosen in order to minimize axial conduction. In mini-channel heat exchangers, it provides higher effectivenesses than good conductors such as copper [4]. The objective of this paper lies in the inversion of the recorded temperature fields on the external faces of this plane channel, which can be measured using an infrared camera, as well as a model of conjugated transfer [5] in the three layers of the system (two walls and the layer of the flow), for :

- estimating the structural parameters of this thermal system (mean velocity and external heat transfer coefficient),
- recovering the temperatures of internal walls and the corresponding wall fluxes from the external temperature distribution and from the external heat transfer coefficient estimated previously,
- retrieving the bulk temperature distribution of the flow in the channel by using a heat balance equation.

2 The studied system and its modelling

Let us consider the following system (figure 1): a laminar flow in a channel of length 2ℓ of thickness e_f, limited by two parallel polycarbonate plates of thicknesses e_1 and e_2. A velocity profile $u(y)$ and a temperature T_∞ are imposed at the entrance of the channel. Two uniform heat flux (φ_{hot} and φ_{cold}) are imposed on a portion $\ell_\varphi = x_2 - x_1 = x_4 - x_3 = 12$ mm of the external faces. The remaining parts of these faces are subject to convective losses to the ambient environment, and the lateral faces are insulated, see figure 1

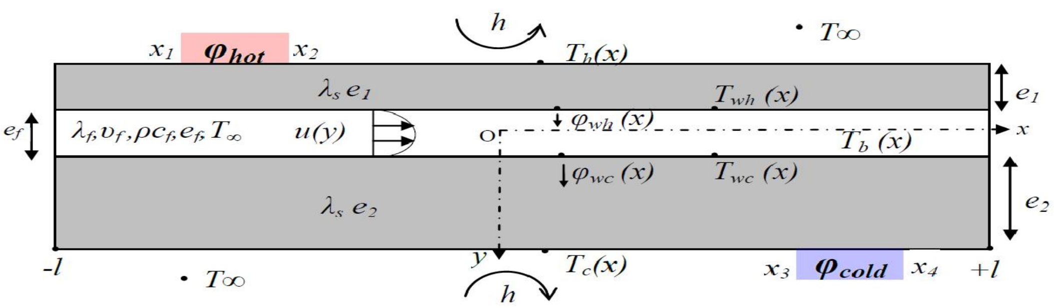

Figure 1: Geometry of mini-channel

The two solid plates are characterized by a thermal conductivity λ_s and a volumetric heat capacity ρc_s. The internal thickness is e_f and the fluid (water) is characterized by a conductivity λ_f, a volumetric heat capacity ρc_f and a kinematic viscosity ν_f, and where $a_f = \frac{\lambda_f}{\rho c_f}$ is the diffusivity.

2.1 Analytical model

The equations describing heat transfer in the mini-channel and in the adjacent parallel polycarbonate plates with the corresponding boundary conditions are given below:

- The heat equation in the walls:

$$\frac{\partial^2 T_s}{\partial x^2} + \frac{\partial^2 T_s}{\partial y^2} = 0 \tag{1}$$

- The heat equation in the fluid:

$$\left(\frac{\partial^2 T_f}{\partial x^2} + \frac{\partial^2 T_f}{\partial y^2}\right) - \frac{u\left(y\right)}{a_f}\frac{\partial T_f}{\partial x} = 0 \tag{2}$$

- Transverse boundary conditions on the external faces, where φ is the heat flux density and $\mathcal{H}$ is the Heaviside step function :

  - at $y = -e_f/2 - e_1$:

$$-\lambda_s \frac{\partial T}{\partial y} = \varphi_{hot}\left[\mathcal{H}\left(x - x_1\right) - \mathcal{H}\left(x - x_2\right)\right] - h\left(T - T_\infty\right) \tag{3}$$

  - at $y = +e_f/2 + e_2$

$$-\lambda_s \frac{\partial T}{\partial y} = -\varphi_{cold}\left[\mathcal{H}\left(x - x_2\right) - \mathcal{H}\left(x - x_3\right)\right] + h\left(T - T_\infty\right) \tag{4}$$

  In real applications, for a channel flow, the input and output thermal boundary conditions (in $x = \pm\ell$) are unknown. So, we consider here a longer virtual channel of length $2L$, with $L \gg \ell$, in order to work on a virtual domain $[-L\ L]$ which includes the real $[-\ell\ \ell]$ interval corresponding to the channel shown in figure 1.

- The lateral boundaries conditions at $x = -L$ for $i = s$ or f become

$$\frac{\partial T_i}{\partial x} = 0 \quad \text{and} \quad T_i = T_\infty \tag{5}$$

- and the solid/fluid interface conditions at $y = \pm e_f/2$ is:

$$-\lambda_s \frac{\partial T_s}{\partial y} = -\lambda_f \frac{\partial T_f}{\partial y} \quad \text{and} \quad T_s = T_f \tag{6}$$

To find the solution of this problem, one can use the Fourier integral transform defined by:

$$\theta\left(\alpha_n, y\right) = \theta_n\left(y\right) = \mathcal{F}\left(T\right) = \int_{-L}^{+L} T\left(x, y\right) e^{-i\alpha_n x} dx \tag{7}$$

where $\alpha_n = \frac{n\pi}{L}$ is the discrete eigenvalue of order n.

Before carrying out the development in Fourier domain of equations (1) and (2), and in order to get an analytical solution, the continuous velocity field $u\left(y\right)$ is transformed into a piecewise constant function, using a set of K fluid sub-layers. The velocity in each layer of thicknesses $e_k = y_k - y_{k-1} = e_f/K$ corresponds to a constant velocity u_k:

$$u\left(y\right) = \frac{3}{2}U\left(1-4\left(\frac{y}{e_f}\right)^2\right) \quad \Rightarrow \quad u_k = \frac{3}{2}U\left(1-\frac{4K}{3e_f^3}\left(y_k - y_{k-1}^3\right)\right) \tag{8}$$

We carry out the development in Fourier transform for the two equations of problems (1) and (2). Here, we write only the development for the equation (2), since solution of the equation (1) is similar:

$$\mathcal{F}\left(\frac{\partial^2 T_f}{\partial x^2}\right) + \mathcal{F}\left(\frac{\partial^2 T_f}{\partial y^2}\right) = \mathcal{F}\left(\frac{u_k}{a_f}\frac{\partial T_f}{\partial x}\right) \tag{9}$$

We develop the three terms of the above equation separately:

- The first term is developed by using a double integration by parts:

$$\mathcal{F}\left(\frac{\partial^2 T_f}{\partial x^2}\right) = \int_{-L}^{+L}\frac{\partial^2 T_f}{\partial x^2}e^{-i\alpha_n x}dx = \left[e^{-i\alpha_n x}\frac{\partial T_f}{\partial x}\right]_{-L}^{+L} + i\alpha_n\left[e^{-i\alpha_n x}T\right]_{-L}^{+L} - \alpha_n^2\theta_{fn} \tag{10}$$

  We assume that $T_i = T_\infty$ and $\partial T_i/\partial x = 0$ at $x = -L$ for $i = s$ or f, see (5). Moreover, it is assumed that there is no heat source and the same external heat transfer coefficient for $x \in [-L\ \ell]$ and $x \in [\ell\ L]$ which yields $T_i = T_\infty$ and $\partial T_i/\partial x = 0$ in $x = L$ as soon as L is large enough with regard to ℓ (because of the external heat loss coefficient h).

  Taking into account this assumption and of the boundary conditions yields:

$$\mathcal{F}\left(\frac{\partial^2 T_f}{\partial x^2}\right) = -\alpha_n^2\theta_{fn} \tag{11}$$

- Concerning the second term, one can write:

$$\mathcal{F}\left(\frac{\partial^2 T_f}{\partial y^2}\right) = \int_{-L}^{+L}\frac{\partial^2 T_f}{\partial y^2}e^{-i\alpha_n x}dx = \frac{\partial^2 \theta_{fn}}{\partial y^2} \tag{12}$$

- And for the last term, one can write:

$$\mathcal{F}\left(\frac{u_k}{a_f}\frac{\partial T_f}{\partial x}\right) = \frac{u_k}{a_f}\int_{-L}^{+L}\frac{\partial T_f}{\partial x}e^{-i\alpha_n x}dx = i\frac{u_k}{a_f}\alpha_n\left[e^{-i\alpha_n x}T\right]_{-L}^{+L} + i\frac{u_k}{a_f}\alpha_n\theta_{fn} \tag{13}$$

  with the boundary conditions at the lateral faces, one obtains:

$$\mathcal{F}\left(\frac{u_k}{a_f}\frac{\partial T_f}{\partial x}\right) = i\frac{u_k}{a_f}\alpha_n\theta_{fn} \tag{14}$$

Finally, after the integral transformation, equations (1) and (2) can be written as follows [5, 3] :

- in the walls:

$$\frac{\mathrm{d}^2\theta_{sn}}{\mathrm{d}y^2} - \alpha_n^2\theta_{sn} = 0 \tag{15}$$

- in the fluid:

$$\frac{\mathrm{d}^2\theta_{fn}}{\mathrm{d}y^2} - \gamma_n^2\theta_{fn} = 0 \tag{16}$$

where $\gamma_n^2 = \alpha_n^2 + i\frac{u_k}{a_f}\alpha_n$.
In the wall, the solution of (15) can be written as:

$$\theta_{sn} = K_1 \sinh(\alpha_n y) + K_2 \cosh(\alpha_n y) \tag{17}$$

Introducing Φ as the Fourier transform of the heat flux φ:

$$\Phi = \mathcal{F}[\varphi] \quad \text{with} \quad \varphi = -\lambda\frac{\partial T}{\partial y} \tag{18}$$

one obtains:

$$\Phi_{sn} = -\lambda\left(K_2\alpha_n \sinh(\alpha_n y) + K_1\alpha_n \cosh(\alpha_n y)\right) \tag{19}$$

where constants K_1 et K_2 are determined by using the boundary conditions at the external hot face if the origin $y = 0$ is located there:

$$K_1 = -\frac{\Phi_h}{\lambda_s\alpha_n} \quad \text{and} \quad K_2 = \theta_h \tag{20}$$

One deduces the input-output system that relies temperatures and fluxes on the extremities of each block:

$$\begin{cases} \theta_h = \cosh(\alpha_n e_1)\,\theta_{wh} + \frac{\sinh(\alpha_n e_1)}{\lambda_s\alpha_n}\Phi_{wh} \\ \Phi_h = (\lambda_s\alpha_n)\sinh(\alpha_n e_1)\,\theta_{wh} + \cosh(\alpha_n e_1)\,\Phi_{wh} \end{cases} \tag{21}$$

The general solution of equations (17) and (19) can be written in the matrix quadrupoles form [3]:

$$\begin{bmatrix}\theta_n \\ \Phi_n\end{bmatrix}_h = \begin{bmatrix} A & B \\ C & D\end{bmatrix}\begin{bmatrix}\theta_n \\ \Phi_n\end{bmatrix}_{wh} \tag{22}$$

where $A = \cosh(\alpha_n e_1)$, $B = \frac{\sinh(\alpha_n e_1)}{\lambda_s\alpha_n}$ and $C = \lambda_s\alpha_n \sinh(\alpha_n e_1)$.

On the same manner, one cane write in each block (solid or fluid) the input-output quadrupole form similar to (24), to finally deduce the global quadrupole form of our system [5]:

$$\begin{bmatrix}\theta_n \\ \Phi_n\end{bmatrix}_h = \boldsymbol{H}_1\boldsymbol{S}_{1n}\left(\prod_{k=1}^{K}(\boldsymbol{F}_{kn})\right)\boldsymbol{S}_{2n}\boldsymbol{H}_2\begin{bmatrix}\theta_n \\ \Phi_n\end{bmatrix}_c \tag{23}$$

where subscripts h and c denote respectively the external hot face and the external cold face, and with

$$\boldsymbol{H}_1 = \boldsymbol{H}_2 = \begin{bmatrix}1 & 0 \\ h & 1\end{bmatrix}, \quad \boldsymbol{S}_{in} = \begin{bmatrix}A_{in} & B_{in} \\ C_{in} & A_{in}\end{bmatrix} \quad \text{and} \quad \boldsymbol{F}_{kn} = \begin{bmatrix}A_{kn} & B_{kn} \\ C_{kn} & A_{kn}\end{bmatrix} \tag{24}$$

and $A_{in} = \cosh(\alpha_n e_i)$, $B_{in} = \sinh(\alpha_n e_i)/(\lambda_s \alpha_n)$ and $C_{in} = (\lambda_s \alpha_n)\sinh(\alpha_n e_i)$, for $i = 1, 2$.

$A_{kn} = \cosh(\gamma_n e_k)$, $B_{kn} = \sinh(\gamma_n e_k)/(\lambda_f \gamma_n)$ and $C_{kn} = (\lambda_f \gamma_n)\sinh(\gamma_n e_k)$, for $i = 1$ to K.

The temperature distribution $T(x, y)$ analytical solution of equations (1) and (2) is obtained through an inverse truncated Fourier transformation with $2N_h$ harmonics:

$$T(x,y) \equiv \frac{1}{2L}\sum_{n=-\infty}^{\infty}\theta_n(y)\,e^{i\alpha_n x} \approx \frac{1}{2L}\sum_{n=-N_h+1}^{N_h}\theta_n(y)\,e^{i\alpha_n x} \tag{25}$$

2.2 Numerical model: simulations for constant flux

At first, our objective is to use the temperature profiles on the external faces and the analytical model to estimate the mean velocity U and the external heat transfer coefficient h. Two types of simulations were carried out here to obtain the temperature fields. The first one uses the commercial code COMSOL [1], and the second presented above uses a quadrupoles model based on the development with Fourier transforms.

In figures (2) and (3), the temperature profiles on the external faces are plotted. They correspond to the nominal values of the parameters of our model given in tables 1 and 2 and to different mean velocities U (see table 3).

h	φ_{hot}	φ_{cold}	T_∞	λ_s	λ_f	ρc_f	ν_f
W.m^{-2}.K^{-1}	W.m^{-2}	W.m^{-2}	°C	W.m^{-1}.K^{-1}	W.m^{-1}.K^{-1}	J.m^{-3}.K^{-1}	m^2.s^{-1}
10	275	-275	20	0.2	0.63	4.1810^3	1.10^{-6}

Table 1: Standard parameters of our simulation.

e_f	e_1	e_2	ℓ	x_1	x_2	x_3	x_4
m	m	m	m	m	m	m	m
10^{-3}	10^{-3}	2.10^{-3}	6.10^{-2}	-3.2510^{-2}	-2.0510^{-2}	2.0510^{-2}	3.2510^{-2}

Table 2: Standard parameters of our simulation.

One can also introduce the Reynolds number Re and the Péclet number Pe as well as M the non-dimensional number introduced in [4] that quantifies the ratio of the heat flow rates transferred by axial conduction in the wall and advective heat transfer in the flow [4, 5]:

$$Re = \frac{2Ue_f}{\nu} \quad \text{and} \quad Pe = \frac{2Ue_f}{a_f} \quad \text{and} \quad M = \frac{\lambda_s e_s}{\rho c_f e_f \ell U} = \frac{2e_s}{\ell}\frac{\lambda_s}{\lambda_f}\frac{1}{Pe} \tag{26}$$

U (m/s)	Re	Pe	M
10^{-3}	1.99	13.96	$4\ 10^{-3}$
10^{-4}	$1.99\ 10^{-1}$	1.396	$4\ 10^{-2}$
10^{-5}	$1.99\ 10^{-2}$	$1.396\ 10^{-1}$	$4\ 10^{-1}$

Table 3: Mean velocity and corresponding non-dimensional numbers.

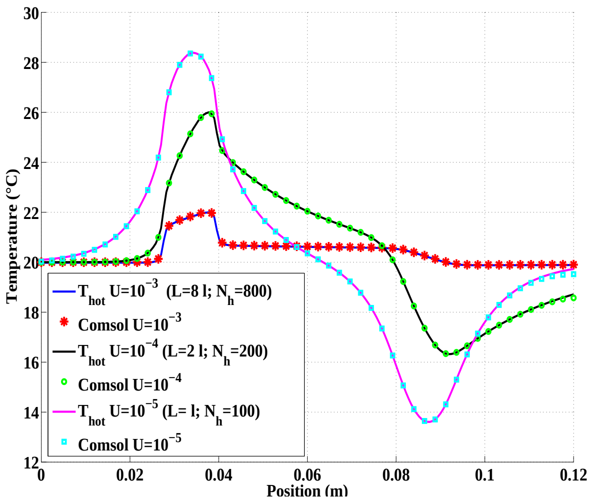

Figure 2: Comparison analytical/numerical temperature on hot face for different mean velocities U (in m/s).

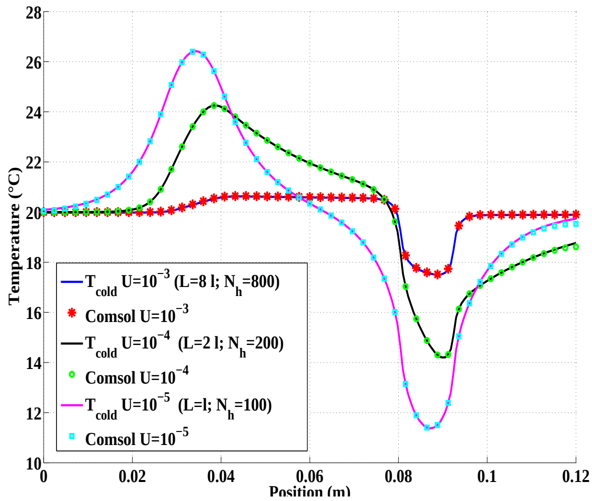

Figure 3: Comparison analytical/numerical temperature on cold face for different mean velocities U (in m/s).

Let us note that we have taken $e_s = e_1$ for the calculation of M in table 3. The last expression of M shows that axial conduction effects disappear for high Péclet numbers, large length of the channel with respect to the thickness of the solid walls ($2e_s \ll \ell$) and for solid walls poorly conductive with respect to the fluid ($\lambda_s \ll \lambda_f$).

One notes in figures 2 and 3 the very good agreement between the temperature profiles calculated by COMSOL code [1] and those obtained by the analytical model with $\frac{L}{N_h} = cte$. A small difference appears at the downstream end of the channel: it can be explained by the short distances between the sources and the insulated ends.

3 Inverse approach

Our first objective is to use the temperature profile at one of the external faces to estimate both the mean velocity of the fluid U and the external heat transfer coefficient h. Before implementing this parameter estimation problem, a sensitivity study has been made for parameters U and h. The four scaled sensitivities on both external faces are defined by [2]:

$$S^*_{\text{hot}U} = U\frac{\partial T_h}{\partial U}, \quad S^*_{\text{cold}U} = U\frac{\partial T_c}{\partial U}, \quad S^*_{\text{hot}h} = h\frac{\partial T_h}{\partial h} \quad \text{and} \quad S^*_{\text{cold}h} = h\frac{\partial T_c}{\partial h} \tag{27}$$

These coefficients are plotted in figures (4) for different mean velocities U (10^{-5}, 10^{-4} and 10^{-3} (m/s)).

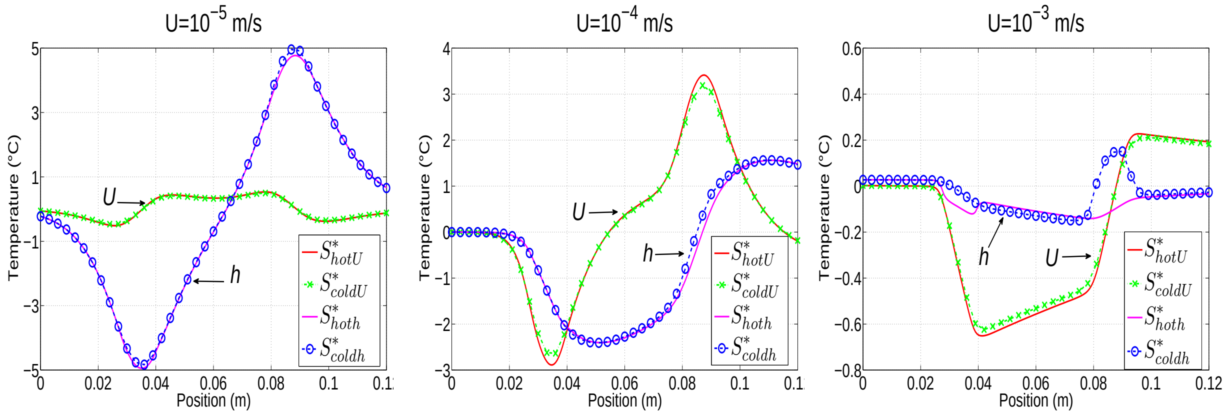

Figure 4: Distribution of scaled sensitivity for different value of U.

The scaled sensitivities on both external faces are almost same (figure 4). For a low mean velocity U, the levels of the scaled sensitivity to the external heat transfer coefficient h are more important than those to the mean velocity U. On the contrary, the levels of scaled sensitivity to U become dominant for high velocities. We can conclude that the higher the velocity the higher advection prevails with respect to conduction in the heat exchange (see the Péclet number levels).

3.1 Estimation of U and h

For the first attempt of inversion we use the data without noise. The estimation is performed through the minimization of a quadratic criterion built on the difference between the analytical temperature profile on the hot face $T_h(x_i)$ for $U = 10^{-5}$ (m/s) and $h = 10$ W.m^{-2}.K^{-1} on $N_x = 200$ points in the $[-\ell\ \ell]$ interval and the analytical model output $T_h(x_i; U, h)$:

$$\mathcal{J}(U, h) = \sum_{i=1}^{N_x} \left(T_h(x_i) - T_h(x_i; U, h)\right)^2 \tag{28}$$

This procedure of minimization uses a method of nonlinear programming based on Trust region algorithm (MATLAB [7, 9]).

For the lowest velocity case, one obtains after minimization $\hat{U} \approx 10^{-5}$ (m/s) and $\hat{h} \approx 10$ (W.m^{-2}.K^{-1}) with relative estimation errors of the order of 2.10^{-7} for U and 3.10^{-6} for h and with a mean quadratic error $\sigma = \sqrt{\mathcal{J}/N_x} = 2.6\ 10^{-5}$ K. Then, one adds a normal and independent noise to the temperature profile $T_h(x)$. This noise is characterized by a standard deviation $\sigma_T = 0.1$ K. For one single estimation, one obtains after minimization $\hat{U} = 9.989\ 10^{-4}$ (m/s) and $\hat{h} = 9.899$ (W.m^{-2}.K^{-1}). The rms residual between the temperature profile on the hot face $T_h(x)$ and the simulated profile $T_h\left(x_i; \hat{U}, \hat{h}\right)$ is of the same order magnitude as the standard deviation of the added noise.

To quantify the quality of the estimation procedure, one can calculate the variance-covariance matrix defined by:

$$cov\left(\hat{\beta}\right) = \sigma_T^2 \left(\boldsymbol{S}^T \boldsymbol{S}\right)^{-1} \tag{29}$$

where $\boldsymbol{S}$ is the sensitivity matrix and $\beta = [U, h]^T$ is the parameter vector. This covariance matrix has diagonal elements which are the variances of $\hat{\beta}_j$'s. They characterize the dispersion (standard deviation) of the estimation $\hat{\beta}$ of parameter β around the expectation of the estimator:

U	relative standard deviation $\sigma_{\hat{U}}/U$	relative standard deviation $\sigma_{\hat{h}}/h$
10^{-3}	2.87×10^{-2}	12.9×10^{-2}
10^{-4}	0.46×10^{-2}	0.48×10^{-2}
10^{-5}	2.06×10^{-2}	0.25×10^{-2}

Table 4: Relative standard deviation for the covariance matrix.

To verify this results, one carries out several tests of inversion with $N_s = 100$ realizations of the added noise. The results in terms of statistical averages $\bar{\hat{U}}$ and $\bar{\hat{h}}$ and standard deviations $s_{\hat{U}}$ and $s_{\hat{h}}$ of the N_s estimations are given in table 5.

U	$\bar{\hat{U}}$	$s_{\hat{U}}/U$	$\bar{\hat{h}}$	$s_{\hat{h}}/h$
10^{-3}	9.9837×10^{-4}	2.4518×10^{-2}	10.1454	8.480×10^{-2}
10^{-4}	9.994×10^{-5}	0.402×10^{-2}	9.9969	0.46×10^{-2}
10^{-5}	1.0009×10^{-5}	1.9625×10^{-2}	10.0013	0.25×10^{-2}

Table 5: Evolution of the estimation results of U and h with the mean velocity U.

All these results show that both parameters can be estimated using measured temperatures.

3.2 Estimation of the boundary conditions at the internal walls

One uses here the analytical model (23) as well as the temperature of the external faces and with the external coefficient of exchange h previously estimated in order to estimate internal wall temperature T_{wh} and T_{wc} and internal wall fluxes φ_{wh} and φ_{wc}. It is an inverse heat conduction problem where the wall temperature profile and flux on both external faces of the system are considered as data (input). By writing now the quadrupolar relationship (23) between the hot face and the internal hot wall, one obtains:

$$\begin{bmatrix} \theta_n \\ \Phi_n \end{bmatrix}_h = \boldsymbol{H}_1 \boldsymbol{S}_{1n} \begin{bmatrix} \theta_n \\ \Phi_n \end{bmatrix}_{wh} \quad \text{therefore} \quad \begin{bmatrix} \theta_n \\ \Phi_n \end{bmatrix}_{wh} = (\boldsymbol{H}_1 \boldsymbol{S}_{1n})^{-1} \begin{bmatrix} \theta_n \\ \Phi_n \end{bmatrix}_h \tag{30}$$

Thus starting from the simulated noisy temperature and the known source on the hot face, one can estimate the Fourier transform of temperature and flux $\begin{bmatrix} \theta_n \\ \Phi_n \end{bmatrix}_h$ for $N_h' \leq N_h$ harmonics (parametrization of the data using model (25)) the boundary conditions at the internal hot wall $T_{wh}(x)$ and $\varphi_{wh}(x)$ are deduced afterwards, see (30).

Starting from inverse Fourier transformation (25), one can write this equation under matrix form :

$$T_{h \text{ or } c} = G\, \theta_{h \text{ or } c} \tag{31}$$

where G is a matrix of dimension $(2N_x, 2N_h)$ and θ the vector of harmonics of dimension $(2N_h)$ which are defined as:

$$G^T = \frac{1}{2L}\exp\begin{bmatrix} i\alpha_1 x_1 & i\alpha_1 x_2 & \cdots & i\alpha_1 x_{2N_x} \\ \vdots & \vdots & \vdots & \vdots \\ i\alpha_{2N_h} x_1 & i\alpha_{2N_h} x_2 & \cdots & i\alpha_{2N_h} x_{2N_x} \end{bmatrix} \quad \text{and} \quad \theta = \begin{bmatrix} \theta_1 \\ \vdots \\ \theta_{N_h} \end{bmatrix} \tag{32}$$

The harmonics vector θ of $2N_h$ dimension is estimated by using least squares method ($\hat{\theta} = \left(G'^T G'\right)^{-1} G'^T T^{\text{noisy}}$) where G' is calculated with $N_h' \leq N_h$ and by incrementing order of θ (that is to say number of harmonics N_h) until reaching one of the stop criteria:

- Mean quadratic error σ_{est} less then $1.1 \times \sigma_T$ where σ_T is the standard deviation of the added or the experiment noise and where $\sigma_{est} = \frac{\sum_{i=1}^{N_x}\left(T_h(x_i) - \hat{T}_h(x_i)\right)^2}{2N_x}$
- Evolution of σ_{est} error between two harmonics is lower than $1\ \%$

For $U = 10^{-5}$ (m/s)) the evolution of σ_{est} function of N_h number of harmonic is plotted in figure 5.

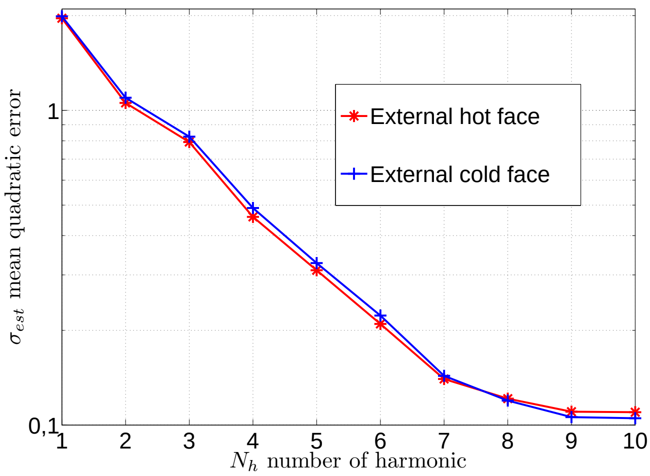

Figure 5: Evolution of σ_{est} function of N_h number of harmonic for $U = 10^{-5}$ (m/s)).

In figure 6, one plots the noisy temperature profile of the external hot face T_h (pseudo-experiment with $\sigma_T = 0.1$ °C) and the parametrized temperature profile $\hat{T}_h$ obtained with $N_h' = 10$ harmonics and also the corresponding temperature residual.

The results of the estimation of the internal walls boundary conditions for $U = 10^{-5}$ (m/s) are now considered. One uses equation (30) that allows to obtain the temperature and flux harmonics on the internal hot wall starting from temperature and flux harmonics on the external hot face. Figure 7 shows the temperature profiles T_{wh} obtained by the analytical model (30) for $N_h = 100$ and by inversion of (30) using the previously parameterized external T_h profile ($N_h' = 10$). The difference (error) between these profiles is also shown on the same figure.

For the cold wall, one can write in a similar manner:

$$\begin{bmatrix} \theta_n \\ \Phi_n \end{bmatrix}_{wc} = \boldsymbol{S}_{2n}\boldsymbol{H}_2 \begin{bmatrix} \theta_n \\ \Phi_n \end{bmatrix}_c \tag{33}$$

The fluxes over external walls (φ_h and φ_c) and internal wall (parametrized φ_{wh} and φ_{wc} and estimated $\hat{\varphi}_{wh}$ and $\hat{\varphi}_{wc}$) are given in figures 8 and 9 (cold face temperature distribution is simulated the same way using equations (30) and (33)).

For both internal walls the errors in the estimation of the flux distribution is quite low.

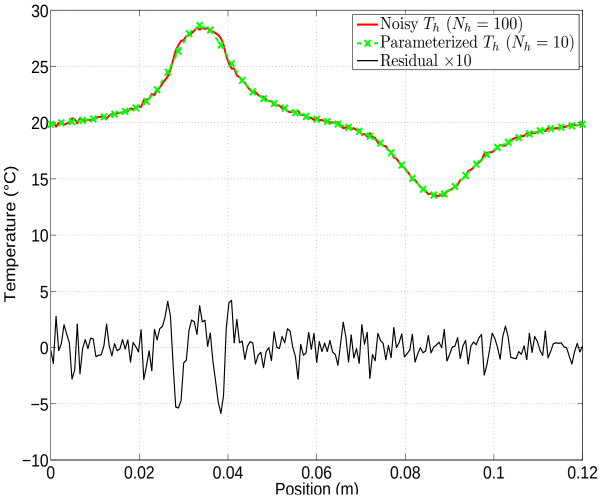

Figure 6: Noisy and parametrized temperatures of the external hot face for $U = 10^{-5}$ (m/s)).

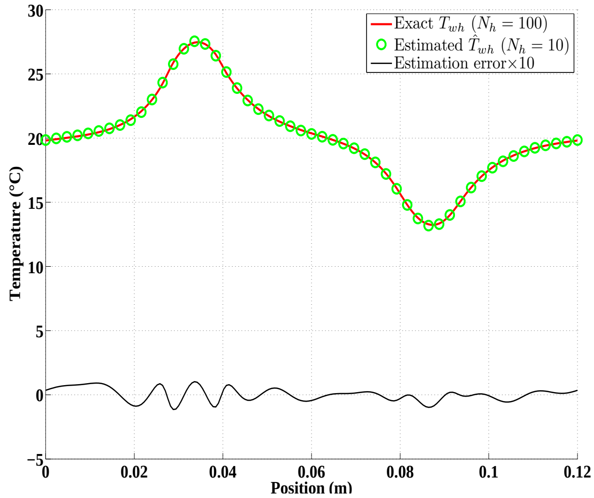

Figure 7: Estimated temperature on the internal hot wall for $U = 10^{-5}$ (m/s)).

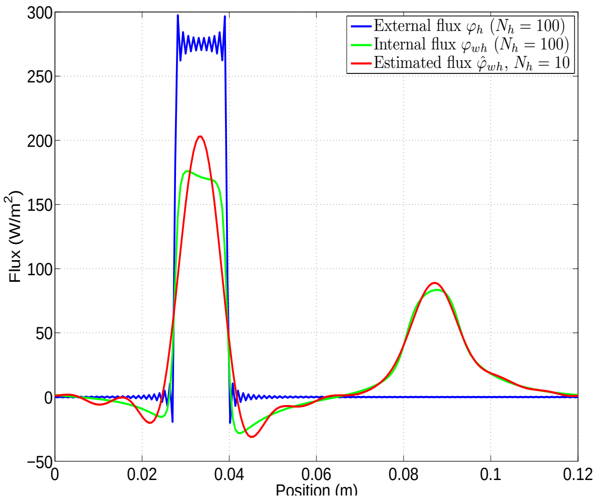

Figure 8: External hot flux (φ_h) and internal hot wall fluxes (φ_{wh} and $\hat{\varphi}_{wh}$).

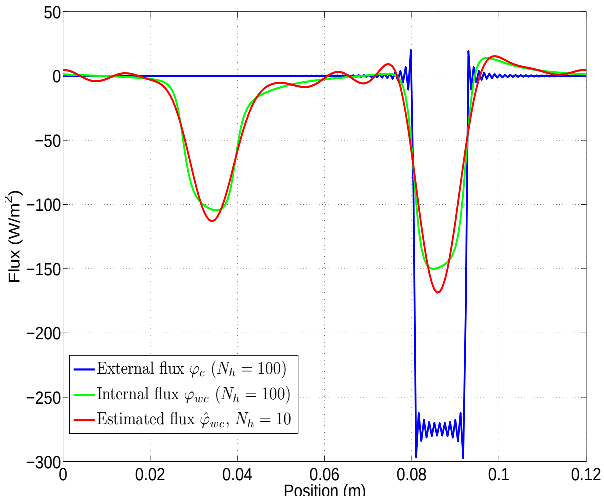

Figure 9: External cold flux (φ_c) and internal cold wall fluxes (φ_{wc} and $\hat{\varphi}_{wc}$).

3.3 Calculation of the bulk fluid temperature

The final objective of this work is to shortcut the notion of internal heat transfer coefficient to recover the bulk temperature $T_b(x)$ of the flow directly. This can be obtained in two different ways:

- By using the quadrupole model and the bulk temperature definition. In 2D channel flow, the bulk temperature $T_b\left(x\right)$ is defined by:

$$T_b\left(x\right) = \frac{1}{Ue_f}\int_0^{e_f} u\left(y\right)T\left(x,y\right)\mathrm{d}y \tag{34}$$

using the decomposition of the fluid layer into K sub-layers previously used to make the velocity field uniform in each layer, one obtains:

$$T_b\left(x\right) = \frac{1}{Ue_f}\sum_{k=1}^{K}\int_{e_{k-1}}^{e_k} u_k\,\bar{T}_k\left(x\right)\mathrm{d}y \quad \text{where } \bar{T}_k\left(y\right) = \frac{1}{2}\left(T\left(x_k,y\right)+T\left(x_{k-1},y\right)\right) \tag{35}$$

therefore:

$$T_b\left(x\right) = \frac{1}{Ue_f}\sum_{k=1}^{K} u_k\,T_k\left(x\right)e_k \tag{36}$$

where $T_k\left(x\right)$ will be calculated the same way as the wall temperatures by using the analytical model:

$$\begin{bmatrix}\theta_n\\ \Phi_n\end{bmatrix}_{y_k} = \left(\boldsymbol{H}_1\boldsymbol{S}_{1n}\left(\prod_{j=1}^{k}\left(\boldsymbol{F}_{kn}\right)\right)\right)^{-1}\begin{bmatrix}\theta\\ \Phi\end{bmatrix}_h \tag{37}$$

- Through a thermal balance in the fluid:

$$\dot{m}c\frac{\mathrm{d}T_b}{\mathrm{d}x} = \left(\varphi_{wh}-\varphi_{wc}\right)p + \lambda S\frac{\mathrm{d}^2T_b}{\mathrm{d}x^2} \tag{38}$$

After Fourier transform, equation (38) become:

$$\dot{m}ci\alpha_n\theta_{bn} = \left(\Phi_{whn}-\Phi_{wcn}\right)p + \lambda Si^2\alpha_n^2\theta_{bn} \tag{39}$$

therfore

$$\theta_{bn} = \frac{1}{\left(\rho ceUi\alpha_n + \lambda e\alpha_n^2\right)}\left(\Phi_{whn}-\Phi_{wcn}\right) \tag{40}$$

hence $T_b\left(x\right)$ is deduced by using an inverse Fourier transformation:

$$T_b(x,y) \approx \frac{1}{2L}\sum_{n=-N_h+1}^{N_h}\theta_{bn}\left(y\right)e^{i\alpha_n x} \tag{41}$$

The obtained fluid bulk temperature for $U = 10^{-5}$ (m/s) with the corresponding external faces temperatures are shown in figure 10.

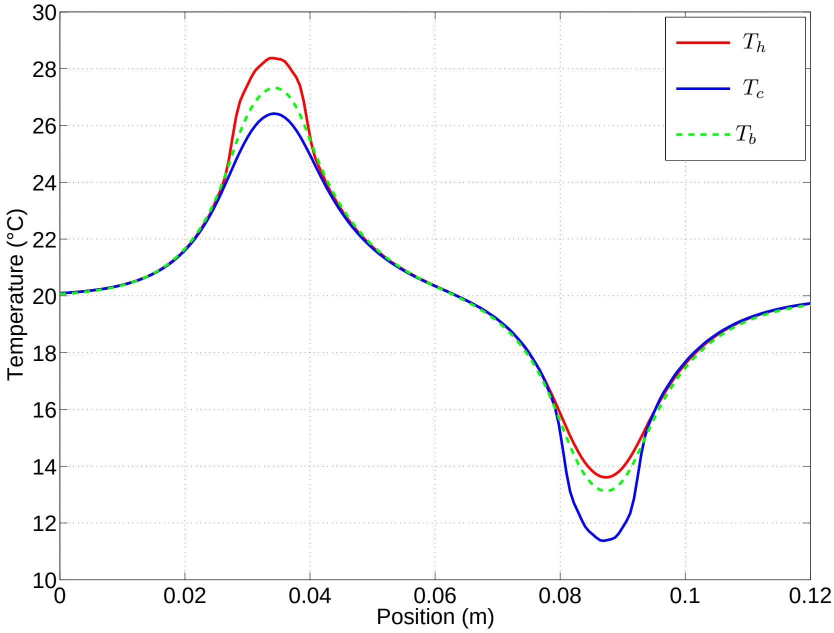

Figure 10: Temperature over external faces and fluid bulk temperature distribution $T_b(x)$ for $U = 10^{-5}$ (m/s).

4 Conclusion

The objective of this preliminary study is a numerical modelling of the flow and heat transfer in a plane mini-channel with a validation of the modelling through an experiment bench where the distribution of the temperature is measured by an infrared camera. It has been presented an analytical model using Fourier transforms that allows the calculation of the conjugated heat transfer inside a mini-channel without the use of any internal heat transfer coefficient. A sensitivity analysis of the temperature distribution to the velocity profile and to the external heat transfer coefficient has been implemented, as well as the inversion of external 1D temperature fields. The next stage will consist to the experimental validation by using the model developed in this study and the infrared thermography in an inverse approach.

References

REFERENCES

[1] Comsol multiphysics version 3.4.

[2] D.Maillet B. Rémy, S. André. Non linear parameter estimation problems: tools for enhancing metrological objectives, lecture l4,. In *Proceeding of Eurotherm Seminar 94: Metti 5 Advanced Spring School Thermal Measurements and Inverse Techniques", Roscoff, Brittany, France,*. Metti 5 Advanced Spring School, June 13-18 2011.

[3] J.C. Batsale A. Degiovanni C. Moyne D. Maillet, S. André. *Thermal quadrupoles: solving the heat equation through integral transforms*. Wiley, 2000.

[4] D. Maillet G. Maranzana, I. Perry. Mini and micro-channels: influence of axial conduction in the wall. *International Journal of Heat and Mass Tranfert*, 47:3993–4004, 2004.

[5] D. Maillet B. Fiers I. Perry, Y. Jannot. Effect of velocity distribution on external wall temperature field for a flat microchannel. *Experimental Heat Transfer*, 23:27–43, 2009.

[6] B. Cetin K.D. Cole. The effect of axial conduction on heat transfer in a liquid microchannel flow. *International Journal of Heat and Mass Transfer*, 54:2542 – 2549, 2011.

[7] MATLAB. *version 7.12.0.635 (R2011a)*. The MathWorks Inc., Natick, Massachusetts, 2011.

[8] G.L. Morini. Single-phase convective heat transfer in microchannels: A review of experimental results. *International Journal of Thermal Sciences*, 43, Issue 7:631–651, 2004.

[9] Y. Yuan. A review of trust region algorithms for optimization, 2007. http://citeseerx.ist.psu.edu/viewdoc/summary?doi=?doi=10.1.1.45.9964.